

引用格式: SONG Ke-xin, JIA Xue-zhi, LI Ji, *et al.* Design on Global Imaging Mode Based on Electronic Rolling Shutter CMOS[J]. *Acta Photonica Sinica*, 2019, 48(8):0804003

宋可心, 贾学志, 李季, 等. 帘幕式 CMOS 全局曝光成像技术[J]. 光子学报, 2019, 48(8):0804003

帘幕式 CMOS 全局曝光成像技术

宋可心¹, 贾学志^{1,2}, 李季¹, 张弘治¹

(1 长光卫星技术有限公司, 长春 130102)

(2 中国科学院长春光学精密机械与物理研究所, 长春 130022)

摘要: 为了消除面阵 CMOS 航空相机高速成像时帘幕快门效应对成像质量的影响, 分析了 CMOS 成像原理, 开展了基于高速中心式机械快门与面阵 CMOS 图像传感器协同工作的全局曝光成像模式研究. 建立了该成像模式下的航空高分辨率成像系统的信噪比模型与前向像移模型, 并基于信噪比模型与前向像移模型论证存在合理的曝光时间参数. 设计了体积小、质量轻、电驱动、曝光时间可准确控制的高速中心式机械快门, 最短曝光时间可达 $1/2\ 000\ \text{s}$, 快门效率最高达 80%. 对采用自主研发的国产 CMOS 图像传感器的航空摄影相机参数进行验证计算, 并进行直升机载人带飞拍摄实验. 影像结果表明: 该成像模式曝光时间参数论证正确, 影像无拉伸、扭曲及拖尾现象, 相机动态传递函数为 0.21 (奈奎斯特截止频率处), 能够满足实际应用需求.

关键词: 卷帘 CMOS; 机械快门; 信噪比; 前向像移

中图分类号: TN432

文献标识码: A

doi: 10.3788/gzxb20194808.0804003

Design on Global Imaging Mode Based on Electronic Rolling Shutter CMOS

SONG Ke-xin¹, JIA Xue-zhi^{1,2}, LI Ji¹, ZHANG Hong-zhi¹

(1 Chang Guang Satellite Technology CO., LTD, Changchun 130102, China)

(2 Changchun Institute of Optics, Fine Mechanics and Physics, Chinese Academy of Science, Changchun 130022, China)

Abstract: In order to eliminate the influence of rolling shutter on image quality in higher speed mapping by a CMOS airborne digital camera, the combination imaging mode of matrix array CMOS and high speed central mechanical shutter is emphatically studied based on CMOS imaging principle. The forward motion model and Signal-to-Noise Ratio (SNR) model of matrix array CMOS resolution imaging system based on the combination imaging mode are proposed and the existence of the corresponding range of exposure is proved under the condition of suitable forward motion and SNR of the airborne digital camera. A small-sized electric and exposure controlled accurately high speed central mechanical shutter is designed with the shortest exposure ($1/2\ 000\ \text{s}$) and the highest efficiency (80%). Finally, the correctness of the right range of exposure is verified by the experimental results of the radiation calibration of an airborne digital camera based on a domestic CMOS image sensor. The experimental data indicates that the parameter proven of combination imaging mode is right and the camera's dynamic MTF at Nyquist frequency (91 lp/mm) is 0.21 which meets the practical application requirement.

Foundation item: The National High Technology Research and Development Program of China (No.2016YFB0500904), the Key Scientific and Technological Research and Development Projects in Jilin Province (No.20170204078G)

First author: SONG Ke-xin (1989-), male, M.D. degree, mainly focuses on aerial camera technology. Email: songkexin1989@163.com

Supervisor (Contact author): JIA Xue-zhi (1980-), male, professor, Ph.D. degree, mainly focuses on overall R&D design of space camera technology. Email: xuezhi0817@163.com

Received: Apr.4, 2019; **Accepted:** May 28, 2019

<http://www.photon.ac.cn>

Key words: Rolling CMOS; Central mechanical shutter; Signal-to-noise ratio; Forward motion
OCIS Codes: 040.1490; 110.5200; 280.4788; 350.4600

0 Introduction

Currently, COMS and CCD image sensor, as two core photosensitive devices of space high-resolution imaging system and the main component of aerial remote camera, are widely used in many fields such as resource survey, terrain mapping and military reconnaissance in the world. Matrix array CCD image sensor is popularized to the field of aerial mapping camera because of its unique hardware design based on global exposure mode. Presently, the more advanced aerial matrix array mapping cameras are made of ZEISS DMC series, Microsoft-Vexcel Ultra-Cam series and Leica RCD series^[1]. However, it cannot be ignored that the complex processing technology, leading to low yield of the product and extremely high price, is not conducive to its wide application. Meanwhile, the complex peripheral circuit of CCD, and the volume, weight and power consumption of CCD image sensor cannot fully meet the current demand for the development of remote sensing camera miniaturization^[2]. Compared with CCD image sensor, COMS image sensor with low cost, high integration, simple peripheral circuit, small volume, low power consumption, is more and more favored by the market^[2-3]. Particularly in aerospace line sweep imaging field, the development of light and small space remote sensing push-pull camera represented by Jilin-1 series satellite provides an excellent opportunity for the application and promotion of CMOS image sensor. It is particularly worth mentioning that, internationally the remote sensing cameras represented by the ADS series line array camera, based on CMOS image sensors, is as good as the CCD area array aerial camera represented by the DMC series^[4].

Although therevolution of domestic airborne remote sensing cameras starts late, the continuous research on linear array CMOS imaging technology by the research institute represented by Changchun Institute of Optics, Fine Mechanics and Physics Chinese Academy of Science, will inevitably promote the development of linear array remote sensing camera^[5-7]. However, in the field of mobile mapping, especially in the matrix array CMOS aerial photogrammetry, the unique curtain exposure mode of CMOS makes images prone to distortion such as stretch and compression, which limits its popularization and application in the field of high-end matrix array aerial photogrammetry^[8]. In order to reduce or eliminate the influence of CMOS Rolling Shutter (RS) on mobile imaging, extrapolation method and RS model method are proposed to repair the image^[9-10], but the effect was not significant.

Therefore, a global exposure imaging mode based on high-speed central mechanical shutter and CMOS working together is proposed in this paper, which fundamentally solves the distortion characteristics of matrix array CMOS image sensor and makes it widely used in the field of matrix array camera. It is of great significance to reduce production costs and improve economic benefits.

1 Principle of CMOS imaging distortion

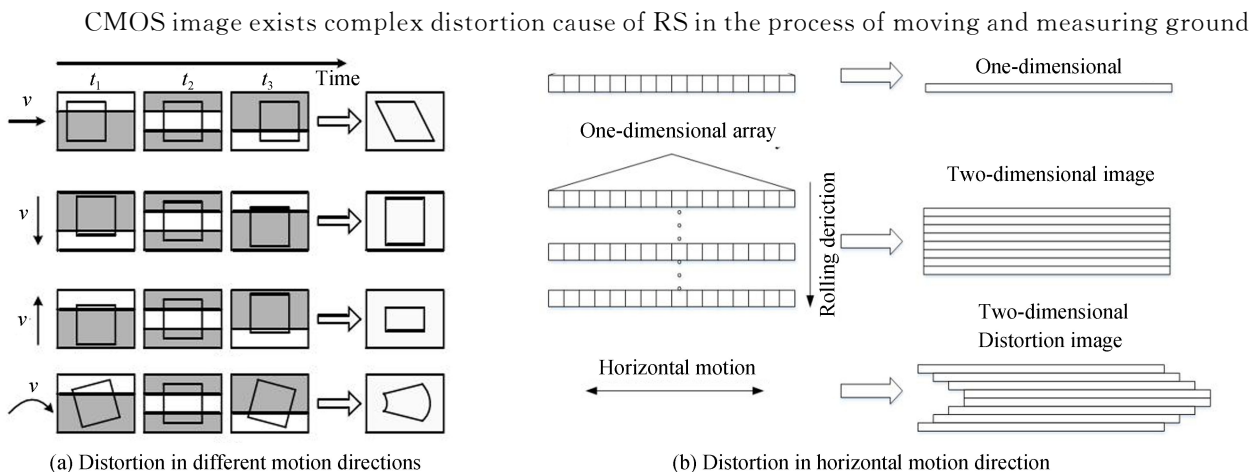


Fig.1 The schematic diagram of distortion generation

objects, as shown in Fig.1(a). Take the horizontal distortion as an example shown in Fig.1(b). After the CMOS first line pixels of exposure at the initial time, the second line pixels are exposed next time, so there is a certain degree of misalignment between the adjacent line of exposure image of the CMOS during the time interval. Until the end of the last line of exposure, the final image is an obliquely stretched image resembling a diamond frame.

2 Cooperative mode of shutter and CMOS

The aerial mapping camera is mainly composed of an optical lens, a high-speed center shutter, an matrix array CMOS image sensor, an inertial measuring device IMU and a positioning system POS, as shown in Fig. 2(a). The imaging mode is that all the CMOS pixels are exposed at a certain moment by controlling the exposure time of each pixel, but nothing can obtain because of no light. Synchronously the high-speed central mechanical shutter opens and all the pixels of the CMOS image sensor can be simultaneously sensitized, effectively eliminating the stretch and compression of the image. The imaging mode is shown in Fig. 2(b). Specifically order:

- 1) Shutter closes completely;
- 2) CMOS turns on line by line, and keeps all lines open;
- 3) Shutter instantly turns on and starts exposure;
- 4) Shutter closes instantly, and exposure ends;
- 5) CMOS sensor turns off line by line, and data reads out line by line;
- 6) One exposure ends.

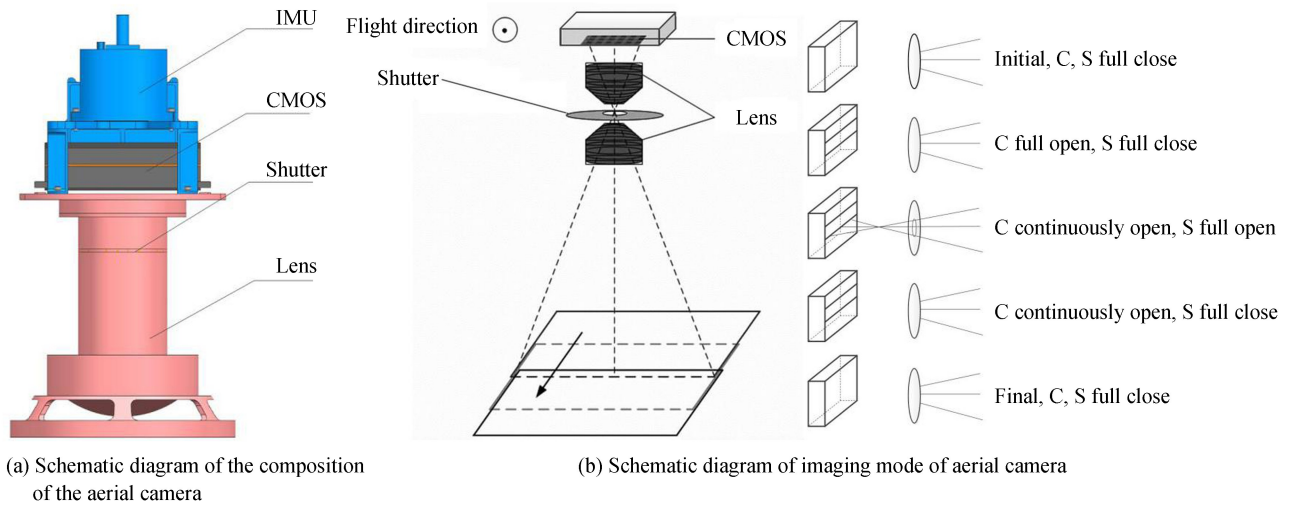


Fig.2 Schematic diagram of aerial camera

The cooperative mode of shutter and CMOS will be conducive to solve the distortion characteristics of matrix array CMOS image sensor. Taken a CMOS (12 000 H×5 000 V active pixels, 10 fps) as example, the distortion of a frame is raised up to 5 m maximum in the process of photoing a 50m/s car. Compared with the cooperative mode of shutter and CMOS, however, a small-sized electric and exposure controlled accurately high speed central mechanical shutter is designed with the shortest exposure (1/2 000 s), and the distortion of a frame is reduced to 0.025 m (originally 0.5% approximately) which can be ignored mostly. The frame rate of cooperative imaging mode, of cause, must be reduce, but it's well enough in practical aerial mapping and there is little influence on photoing to moving objects.

3 Argument of exposure time

Image resolution is reduced in the process of aerial photography because of relative motion. Optical, electronic or mechanical forward motion compensation methods are used in most aerial mapping cameras to improve the imaging resolution. On the premise of ensuring the imaging resolution, reducing the overall quality and improving the reliability of the mapping camera, this camera adopts the cooperative work of high-speed central shutter and matrix array CMOS to eliminate the influence of forward image motion on

the image quality.

3.1 Exposure time based on SNR

The pupil light flux of optical system can be represented as Eq.(1)

$$\varphi_{\lambda 0} = \alpha \beta L_{\lambda} \tau_{\alpha}(\lambda) A_0 \quad (1)$$

where, L_{λ} , $\alpha\beta$, τ_{α} , A_0 respectively represent target pupil radiance, target stereo angle, atmospheric transmittance, pupil area of optical system. The sensor collecting light flux can be represented as Eq.(2)

$$\varphi_{\lambda d} = \alpha \beta L_{\lambda} \tau_{\alpha}(\lambda) A_0 \tau_0(\lambda) \quad (2)$$

where, τ_0 represents optical system transmittance. So sensor signal electron number can be represented as Eq.(3)

$$S_e = \left[\pi A_d t_{\text{int}} / (4F^2 h c) \right] \int_{\lambda} \lambda \tau_{\alpha}(\lambda) \tau_0(\lambda) L_{\lambda} \eta_{\lambda} d\lambda \quad (3)$$

where, A_d , t_{int} , F , h , c , λ , η_{λ} represent pixel size, effective exposure time, camera parameters, Planck constant, light speed, optical wavelength, photoelectric conversion efficiency, respectively. And the sensor noises electron number can be represented as Eq.(4)

$$N_e = \sqrt{\sigma_{\text{rms}}^2 + \sigma_{\text{dark}}^2 + \sigma_{\text{shot}}^2} \quad (4)$$

where, σ_{rms} , σ_{dark} , σ_{shot} represent read noise, dark current noise, particle noise, respectively. So the SNR can be represented as Eq.(5)

$$\text{SNR}(t_{\text{int}}) = S_e / N_e = S_e / \sqrt{S_e + \sigma_R^2 + D_e} \quad (5)$$

3.2 Exposure time based on forward image motion

The influence of forward image motion for image resolution is relative to camera parameters and flight parameters. The ground pixel resolution can be represented as Eq.(6), The pixel size can be represented as Eq.(7)

$$R = \delta H / f \quad (6)$$

$$\delta = f v_s t_{\text{int}} / H = f k t_{\text{int}} \quad (7)$$

where, R , H , f , δ , v_s , k represent pixel resolution, flight height, focal length, pixel size, velocity, and velocity to height ratio, respectively. In order to keep pixel resolution effective, the practical forward image motion must be lower than half of pixel resolution as Eq.(8)

$$\delta \cdot (t_{\text{int}}) \leq \delta / 2 \quad (8)$$

where, $\delta \cdot$ represents forward image motion. Ground sampling distance is determined by the focal length, velocity/height ratio and exposure time. Eqs. (5) and (8) claim that by optimizing the optical system and the ratio of velocity to height reasonably, there must be a reasonable exposure time interval, and satisfy the requirements of sensor signal-to-noise ratio and image motion. The radiance of ground target entering pupil of optical system is mainly related to solar altitude angle, the reflectance of ground target and atmospheric transmittance. The radiance of ground targets is calculated by LOWTRAN software, as shown in Table 1.

Table 1 The ground targets radiance($\text{W} \cdot \text{m}^{-2} \cdot \text{sr}^{-1}$)

Solar altitude angle		10°	30°	50°	60°	70°
		Surface reflectance				
0.05		3.68	7.26	9.85	10.95	11.85
0.1		4.13	9.50	13.7	15.46	16.81
0.2		5.03	14.04	21.56	24.53	26.81
0.4		6.90	23.35	37.50	42.95	47.06

The optimum exposure time distribution is calculated based on engineering experience by SNR formulas, the ground targets radiance and reflectivity of different ground objects, as shown in Table 2. Meanwhile, the relation between pixel resolution, velocity-height ratio and exposure time is shown in Table 3.

The optimum exposure time interval is 0.4~1.1 ms based on the average surface features reflectance of 0.3, shown in Table 2, which is accord with the relation of R , K and t_{int} , shown in Table 3. Meanwhile, the maximum exposure time can be raised to 7 ms to adapt the low-light condition.

Table 2 Exposure time distribution(ms)

Solar altitude angle		10°	30°	50°	60°	70°
		Surface reflectance				
0.05		4.9	2.5	1.8	1.7	1.5
0.1		4.4	1.9	1.3	1.2	1.1
0.2		3.6	1.1	0.8	0.7	0.7
0.4		2.6	0.8	0.5	0.4	0.4

Table 3 The relation of R, K and t_{int}

R	K	t_{int}/ms
0.05	(0.06~0.1)	≤ 2.30
0.1	(0.03~0.06)	≤ 4.58
0.2	(0.02~0.03)	≤ 6.88

4 High speed center shutter

According to the structure, the existing aerial photography shutters can be classified into three types: center type, louver type and curtain type^[11-12]. In order to eliminate imaging distortion, the central shutter is chosen and placed in aperture bar to reduce the volume of the center shutter and improve efficiency. For the sake of adapting to different illumination and obtaining appropriate image overlap rate and a wide range of exposure, the central mechanical shutter minimum effective exposure time key technology is broken through by electrically driven. It is mainly composed of a rotating electromagnet 1, four blades 2, a dial 3, two photoelectric switches and driving circuit, as shown in Fig.3. Its working principle is that the rotating electromagnet will produce a step response at electrified instant, as shown in Fig.4, in which the blade will be driven very quickly to complete the opening and closing action in a 0.5 ms instant.

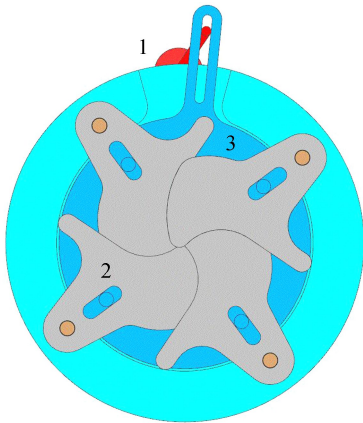


Fig.3 Shutter structure model

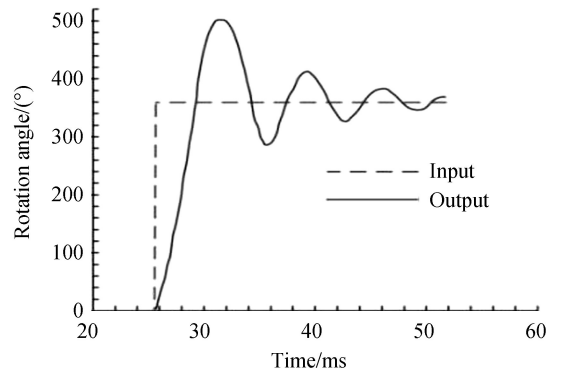


Fig.4 Step response curve of electromagnet

In order to facilitate the analysis, the following two assumptions are proposed in the mathematical modeling:

- 1) Ignoring the effect of load on the output torque of electromagnet.
- 2) Ignoring the effect of friction.

Theoretical model of mechanical shutter is shown in Fig.5.

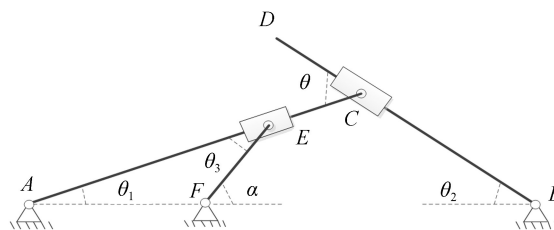


Fig.5 Theoretical model of mechanical shutter

The step response curve as shown Fig.4 can be fitted and represented by time parameter t polynomial, as shown Eq.(9)

$$\alpha = f(t) \quad t_0 \leq t \leq t_0 + 3 \quad (9)$$

where, α, t , represent rotating electromagnet output angle, time parameter, respectively. The relationship between the turning angle of electromagnet and dial, as shown in Fig.5, can be represented as Eq.(10)

$$\sin \alpha / |AE| = \sin \theta_1 / |EF| = \sin \theta_3 / |AF| \quad (10)$$

$$\alpha = \theta_1 + \theta_3 \quad (11)$$

where, $|AE|, |EF|, |AF|, \theta_1, \theta_3$ respectively represent length variable, the effective motion length of rotating electromagnet, distance between the center of rotating electromagnet and dial, the turning angle of dial, and the angle between rotating electromagnet and dial. Eqs.(10), (11)are deduced to Eq.(12)

$$\tan \theta_1 = \frac{\sin \theta_1}{\cos \theta_1} = \frac{\sin \alpha}{(|AF|/EF + \cos \alpha)} \quad (12)$$

Assuming

$$\sin \theta_1 = k \sin \alpha \quad (13)$$

By optimizing the value of $|AF|/|EF|$, the coefficient k can be obtained.

The relationship between the turning angle of blade and dial can be represented as Eq.(14)

$$\sin \theta / |AB| = \sin \theta_1 / |BC| = \sin \theta_2 / |AC| \quad (14)$$

$$\theta = \theta_1 + \theta_2 \quad (15)$$

where, $|AB|, |BC|, |AC|, \theta_2, \theta$ respectively represent the distance between the rotating centre of electromagnet and dial, length variable, the radius of dial, the turning angle of blade, the angle between dial and blade. Eqs.(14),(15)are deduced to Eq.(16)

$$\tan \theta_2 = \frac{\sin \theta_1}{(|AB|/AC - \sin \theta_1)} \quad (16)$$

Put Eq.(13) into Eq.(16), and the relationship between the turning angle of electromagnet and blade can be represented as Eq.(17)

$$\tan \theta_2 = \frac{k \sin \alpha}{[|AB|/AC - k(|AF|/EF + \cos \alpha)]} \quad (17)$$

Size optimization is one of the most important topology optimization method, especially used in structure optimization. By structure optimization as shown Eq.(17), the boundary condition as shown in Eq.(18) can be obtained and the shortest 0.5 ms instant achieved.

$$\phi \leq \theta_2 \quad (18)$$

Shutter efficiency is an important index in evaluating shutter parameters. The shutter with higher efficiency is able to ensure the image quality of the camera.

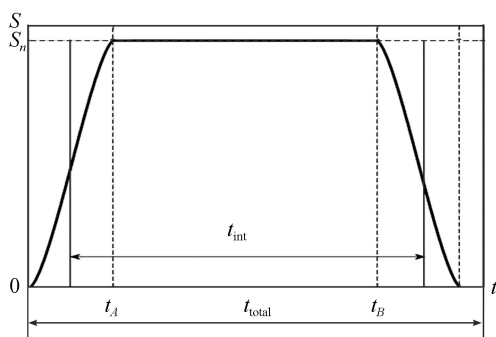


Fig.6 Shutter characteristic curve

The shutter characteristic curve is shown as Fig. 6. The shutter efficiency formula is as follows

$$\eta = t_{\text{int}} / t_{\text{total}} \approx 1 - (t_A + t_B) / 2t_{\text{total}} \quad (19)$$

where, $\eta, t_{\text{total}}, t_A, t_B$, respectively represent the shutter efficiency, real exposure time, shutter open time, shutter close time. The parameter t_A and t_B are mostly equal to nature which are designed to change from 0.1 ms to 1 ms with the precision of 0.05 ms through a high-performance electric circuit. So the shutter efficiency of aerial mapping camera can reach 80% approximately in the abstraction theory.

4.1 Shutter exposure time test

The exposure time of the electrically driven high-speed center shutter is tested using a Thousand-eye Wolf high-speed camera with 5 000 Hz frame rate, as shown in Fig.7. The electrically driven high-speed central shutter completes an exposure cycle once within about 0.5 ms (the time interval corresponding to Fig.8(c) and Fig.8(a)) screening the test image frame by frame. The exposure time test results reach the design expectation, as shown in Fig.8.



Fig.7 Shutter exposure time test

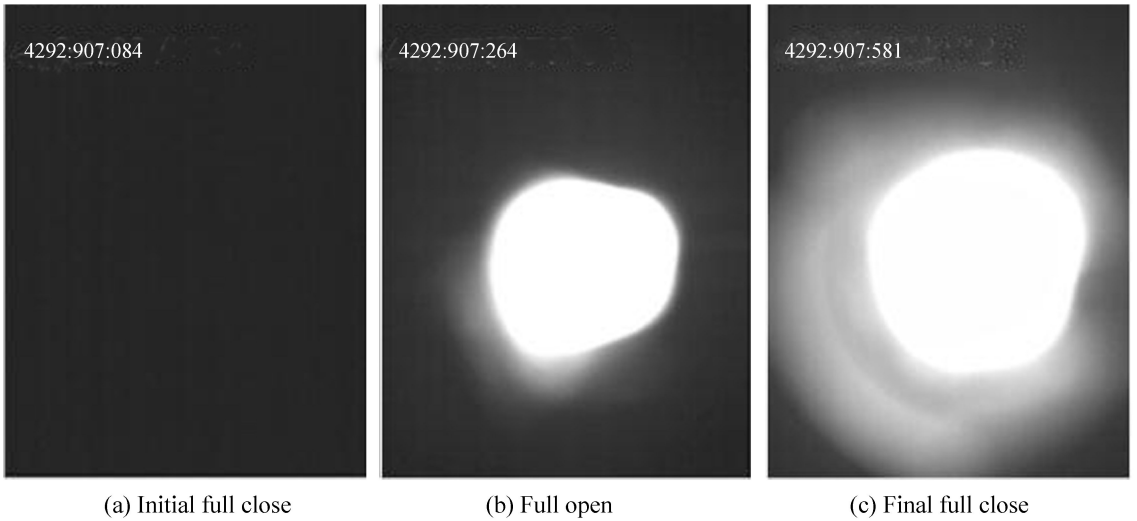


Fig.8 Test image

The shutter efficiency of self-research camera is obtained based on SNR ratio of the images taken by a single CMOS camera and self-research camera separately in the laboratory. The practical exposure time is 0.5 ms. SNR can be calculated respectively on the image and SNR can be obtained with unit of dB through formula as follows

$$\text{SNR} = 20 \times \lg(\text{signal}/\text{noise}) \quad (20)$$

The shutter efficiency of self-research camera is 80% approximately. The center shutter is driven by circuit meaning that the process of exposure is stable and controllable. The accuracy of exposure time is 10^{-2} ms. Consideration for image joints, the influence of distortion for pixel resolution can be ignored mostly if distortion is less than 1/3 of pixel resolution. Under the condition of typical 0.05 m pixel resolution, the distinct reduction of pixel resolution can be created if the speed of relative movement reaches 166 m/s. It does not, however, happens practically. So the accuracy of exposure time is well enough and acceptable.

5 Imaging experiment test

At afternoon 2:00 pm in June 15, 2018, mi171 helicopter equipped with self-research matrix array aerial camera system is used to carry out flight test to verify the imaging effect in the test area of Dunhua city, Jilin province. Fig.9 shows a typical clean and sharp image taken by self-research camera. The

distribution of resident houses and the structure of the village's main roads could be well revealed and the stretch, compression and distortion of image caused by the CMOS shutter effect disappear, thus proving the correctness and effectiveness of the global exposure imaging mode of the high speed central mechanical shutter and matrix array CMOS sensor working together. Significantly, compared with major ADS80 camera aerial image shown as Fig.10, MTF is calculated by using the slant edge method^[13] according to the imaging characteristics of self-research camera. The self-research camera's dynamic MTF at Nyquist frequency (91 lp/mm) is 0.21, which meets the practical application requirement that dynamic MTF should be better than 0.15, although it's less than ADS80's MTF shown in Fig 11.



Fig.9 Self-research camera aerial image

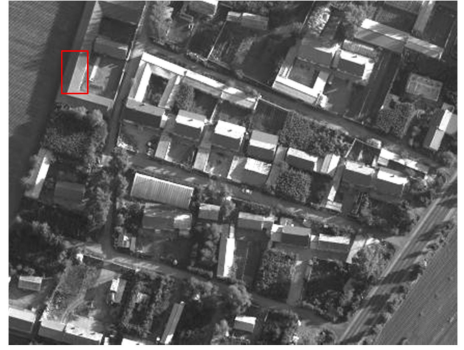


Fig.10 ADS80 aerial image

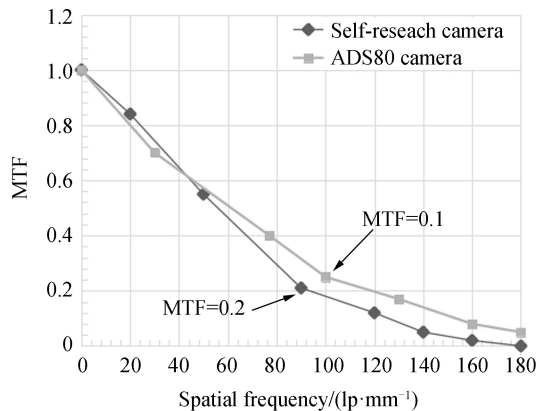


Fig.11 Dynamic modulation transfer function curves

6 Conclusion

The higher cost performance is the constant pursuit of aerial mapping enterprises and represents the development direction of aerial remote sensing to a certain extent. This paper proposes a global exposure imaging mode based on rolling shutter CMOS and high speed central mechanical shutter, which solves the image distortion effectively, and designs a key technology of high speed electric center-type mechanical shutter with the 0.5ms fastest exposure time and the 80% maximum efficiency. Finally, a good imaging effect is obtained and the self-research camera's dynamic MTF at Nyquist frequency (91 lp/mm) is 0.21, which meets the practical application requirement. It is conducive to promote the application of roller shutter CMOS in the field of aerial matrix array remote sensing and mapping.

References

- [1] LIU Xian-lin, DUAN Fu-zhou, GONG Hui-li. Aerial development achievements and future prospects of photography technology[J]. *Frontier Science*, 2007, **3**: 10-14.
- [2] ZHU Qi-xiang. CCD imaging sensor[J]. *Modern Physics*, 2009, (6): 8-11.
- [3] ABBAS E, HELMY E. CMOS Image sensor [J]. *IEEE Circuits & Devices Magazine*, 2005: 6-20.
- [4] JOHN C. Comparison of leica ADS40 and Z/I imaging DMC high-resolution airborne sensors[C]. SPIE, 2005, **5655**: 271-280.
- [5] WANG Chao. Research on the key technology of compact three line array aerial camera[D]. University of Chinese Academy of Sciences, 2017.

- [6] LAN Tai-ji, Research on high-dynamic-range and high sensitivity optical remote sensing imaging method for digital TDI CMOS[D]. University of Chinese Academy of Sciences, 2018.
- [7] MA Fang-yuan, WANG Yue-ming. Development and application of the light and small CMOS hyperspectral camera[J]. *Optics & Optoelectronic Technology*, 2016, **4**(16): 85-88.
- [8] JIA Ping, ZHANG Ye, WAN Lei. Effect of aircraft attitude on imaging of CMOS aerial cameras[J]. *Optics and Precision Engineering*, 2016, **24**(1): 204-209.
- [9] WAN Lei. Research on key technologies of CMOS with rolling shutter in aviation application[D]. University of Chinese Academy of Sciences, 2016.
- [10] SUM Y, LIU G. Rolling shutter distortion removal based on curve interpolation[J]. *IEEE Transactions on Consumer Electronics*, 2012, **58**(3): 1045-1050.
- [11] ӘАКАӘННОВ Н. The shutter of aerial camera[M]. Beijing : Science Press, 1974.
- [12] LENG Xue, ZHANG Hong-wen, LIU Ming. Design of large format focal-plane shutter with high frame-frequency and orthogonalit[J]. *Optics and Precision Engineering*, 2011, **19**(11): 2631-2635.
- [13] VIALLEFONT F, DOMINIQUE L. Improvement of the edge method for on-orbit MTF measurement[J]. *Optics Express*, 2010, **18**(4): 3531-3545.